Journal of Endourology. Aug 2018; Vol.32(8) pp.685-691.
https://www.liebertpub.com/doi/pdfplus/10.1089/end.2018.0326

A User-Friendly Application to Automate CT Renal Stone Measurement

Software download: http://urobotics.urology.jhu.edu/share/rsm/

Justin B. Ziemba, MD,[1,2] Pan Li, MS,[1] Rishab Gurnani, BS,[1] Satomi Kawamoto, MD,[3] Elliot K. Fishman, MD,[3] George Fung, PhD,[4] Wesley W. Ludwig, MD, MS,[1] Dan Stoianovici, PhD,[1] and Brian R. Matlaga, MD, MPH[1]

Abstract

Introduction: CT is the gold standard for visualizing renal and ureteral calculi. CT three-dimensional reformatting allows for automatic, accurate, and reliable measurement of stone size, volume, density, and location. In this study, we aimed to develop and test a software platform capable of calculating a battery of clinically important urinary stone parameters at the point-of-care (POC).

Methods: The syngo Calcium Scoring (Siemens Corporation) algorithm was modified to identify calcium-based stones using an attenuation threshold (250 HU) within a region of interest. Information automatically obtained after reconstruction included voxel sum and calculated volume, maximum diameter, largest diameter in the *x*, *y*, and *z* planes, cumulative diameter, distribution of attenuation in HU, and position relative to the skin for calculation of the skin-to-stone distance (SSD). This algorithm was packaged into a stand-alone application (MATLAB 9.1). From April 2017 to May 2017, all patients undergoing a noncontrast CT of the abdomen or the abdomen and pelvis at the Johns Hopkins Hospital were eligible for inclusion in this validation cohort.

Results: A total of 55 index renal stones were included. The mean volume calculated by voxel sum was 216.53 mm^3 (standard deviation [SD] ±616.19, range 1.50–4060.13). The mean volume calculated using the Ackermann's formula and for a sphere was 232.96 mm^3 (SD ±702.65, range 1.24–4074.04) and 1214.63 mm^3 (SD ±4233.41, range 1.77–25,246.40), respectively. The mean largest diameter in any one direction was 6.95 mm (SD ±7.31, range 1.50–36.40). The maximum density of the stones ranged from 164 to 1725 HU. The mean SSD at the shortest possible point was 14.19 cm (SD ±6.13, range 6.67–31.28).

Conclusions: We developed a stand-alone platform with a simple easy-to-use interface, which will allow any user the ability to calculate a battery of clinically important urinary stone parameters from CT imaging at the POC. This program is now freely available online.

Keywords: multidetector CT, kidney calculi, image processing, computer-assisted

Introduction

Renal stone disease is relatively common with an estimated overall prevalence of nearly 9% of the U.S. population.[1] A significant proportion of these individuals will experience a symptomatic stone event during their lifetimes,[2] often necessitating imaging to confirm the diagnosis.[3] CT is now considered the gold standard for visualizing calculi along the entire urinary tract.[4,5]

Although CT is incredibly accurate, calculating stone characteristics such as size, volume, density, and location remains cumbersome to perform and inconsistently applied across both clinical care and the reporting of research outcomes.[6] Despite this difficulty, the importance of these parameters for appropriate patient counseling and treatment selection cannot be understated.[7–9]

Traditionally, only stone size is calculated, often in only a single dimension using computer-aided manual calipers performed either by the radiologist or by the urologist.[6,10] The volume of the stone can then be derived from these dimensions by inputting them into a formula. The disadvantage of this approach is that no formula (sphere, ellipsoid, etc.) perfectly matches that of an irregular renal or ureteral stone.[11] Furthermore, the measurements performed are not always exact or reproducible.[12] However, with the introduction of CT three-dimensional (3D) reformatting, computer-aided tools, and

[1]Brady Urological Institute and Department of Urology, Johns Hopkins School of Medicine, Baltimore, Maryland.
[2]Division of Urology, Department of Surgery, Perelman School of Medicine, University of Pennsylvania, Philadelphia, Pennsylvania.
[3]Department of Radiology, Johns Hopkins School of Medicine, Baltimore, Maryland.
[4]Siemens Healthineers, Siemens Medical Solutions USA, Inc., Malvern, Pennsylvania.

algorithms, it is now possible to measure the size, volume, density, and the relative location of the stone directly from the image metadata.

Acquiring clinically important information directly from imaging metadata is not a new concept, but one, which was pioneered in cardiology for coronary artery calcium scoring.[13] Since that original application, it has been extended, at least in a limited capacity to calculate renal stone volume.[11,12,14–17] Despite the promise of this automation to provide accurate clinically relevant stone parameters, it has yet to gain popularity. We believe that this is in large part due to the lack of a freely available, user-friendly software package capable of analyzing CT imaging data. To fill this void, we developed a stand-alone platform with a simple easy-to-use interface, which would allow any user the ability to calculate a battery of clinically important urinary stone parameters at the point-of-care (POC).

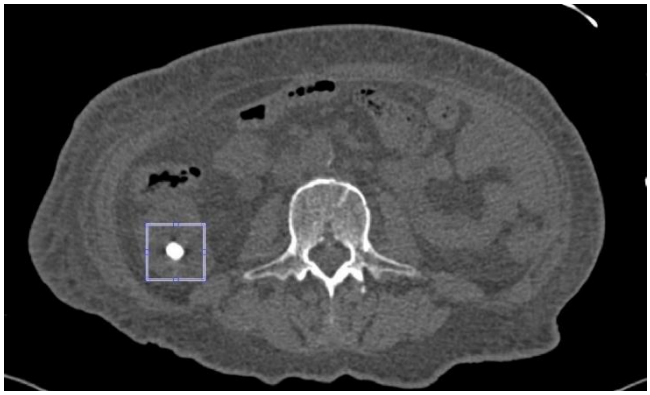

Fig. 1. The box highlights the index renal stone on a single representative CT slice.

Methods

CT imaging

All CT imaging were performed on the SOMATOM Definition Flash CT Scanner (Siemens Corporation, Washington, DC). The CT protocol was set at 120 kVp with a reconstructed 0.5 mm slice thickness. All scans of the abdomen and pelvis without contrast were performed.

Segmentation algorithm

The syngo Calcium Scoring (Siemens Corporation) algorithm was modified to identify calcium-based stones using an attenuation threshold within a region of interest (ROI). Each unique stone does require a separate ROI. An initial attenuation threshold of 250 HU was selected to ensure as much as possible that the stone remains as a single object during region growing, while eliminating adjacent soft tissue. Body habitus has no influence on the segmentation of the stone as long as the correct ROI is defined. However, slice thickness of the scan will have an impact on segmentation accuracy, as thinner slices will provide greater detail of the underlying anatomy. To facilitate even greater accuracy in the segmentation of the stones, the attenuation threshold was set as an adjustable value on the user interface. The segmented binary images were obtained, followed by an automatic reconstruction using marching cubes algorithm. Initial isovalue (ISO) value was selected as 0.4 to make sure the reconstructed stone has a smooth surface. Similarly, the ISO value was set as a controllable parameter to adjust the reconstructed effect. From the reconstructed region, information is automatically derived, which includes voxel sum and calculated volume, maximum diameter, largest diameter in the *x*, *y*, and *z* planes, cumulative diameter, distribution of attenuation in HU, and position relative to the skin for calculation of the skin-to-stone distance (SSD). It will even calculate these parameters for branched irregularly shaped stones (Fig. 3).

User application

This algorithm was packaged into a stand-alone application (MATLAB 9.1; Natick, MA). The application was developed on a Windows 10 64-bit PC and runs on either Windows 64-bit or macOS (Apple Inc.) operating systems. The MATLAB program is not required to run the application as it is exported as a stand-alone executable application. The application allows for easy import of Digital Imaging and Communications in Medicine (DICOM) images directly from picture archiving and communication system (PACS) or other file source (Fig. 1). The program requires all images from a given scan to perform the segmentation. Once the files are imported, the user-friendly interface allows for rapid selection of the ROI (Fig. 2) to generate the reconstructed stone (Fig. 3). If this is not satisfactory, then it is possible to manually modify the attenuation threshold or reconstruction parameters to generate a closer fit to the visualized stone. The user-friendly interface is shown in Figure 4. Once reconstructed, the output data are clearly displayed and available

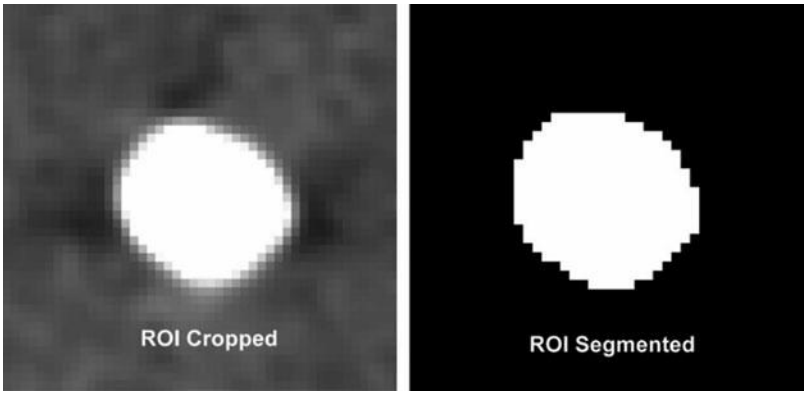

Fig. 2. Index renal stone selected, cropped, and segmented. ROI = region of interest.

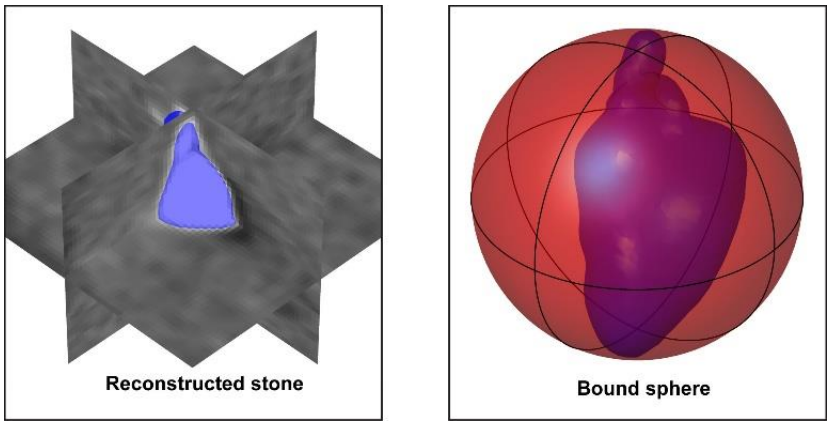

Fig. 3. Reconstructed index renal stone and its bound sphere.

for export as a table. Full versions of the program for Windows 64-bit and macOS (Apple Inc.) operating systems are available online (http://urobotics.urology.jhu.edu/share/rsm).

Study population

From April 2017 to May 2017, all patients undergoing a noncontrast CT of the abdomen or the abdomen and pelvis at the Johns Hopkins Hospital were eligible for inclusion. At the conclusion of the 1-month eligibility period, natural language processing was utilized to identify dictated radiology reports, which included the phrase ''renal stone.'' The images of these patients were then reviewed by the study team to confirm that a renal stone was visible. If a renal stone was confirmed, then the imaging study was included in the final cohort.

Analysis

Each patient's CT scan was extracted from PACS in de-identified DICOM format and then opened with the stone

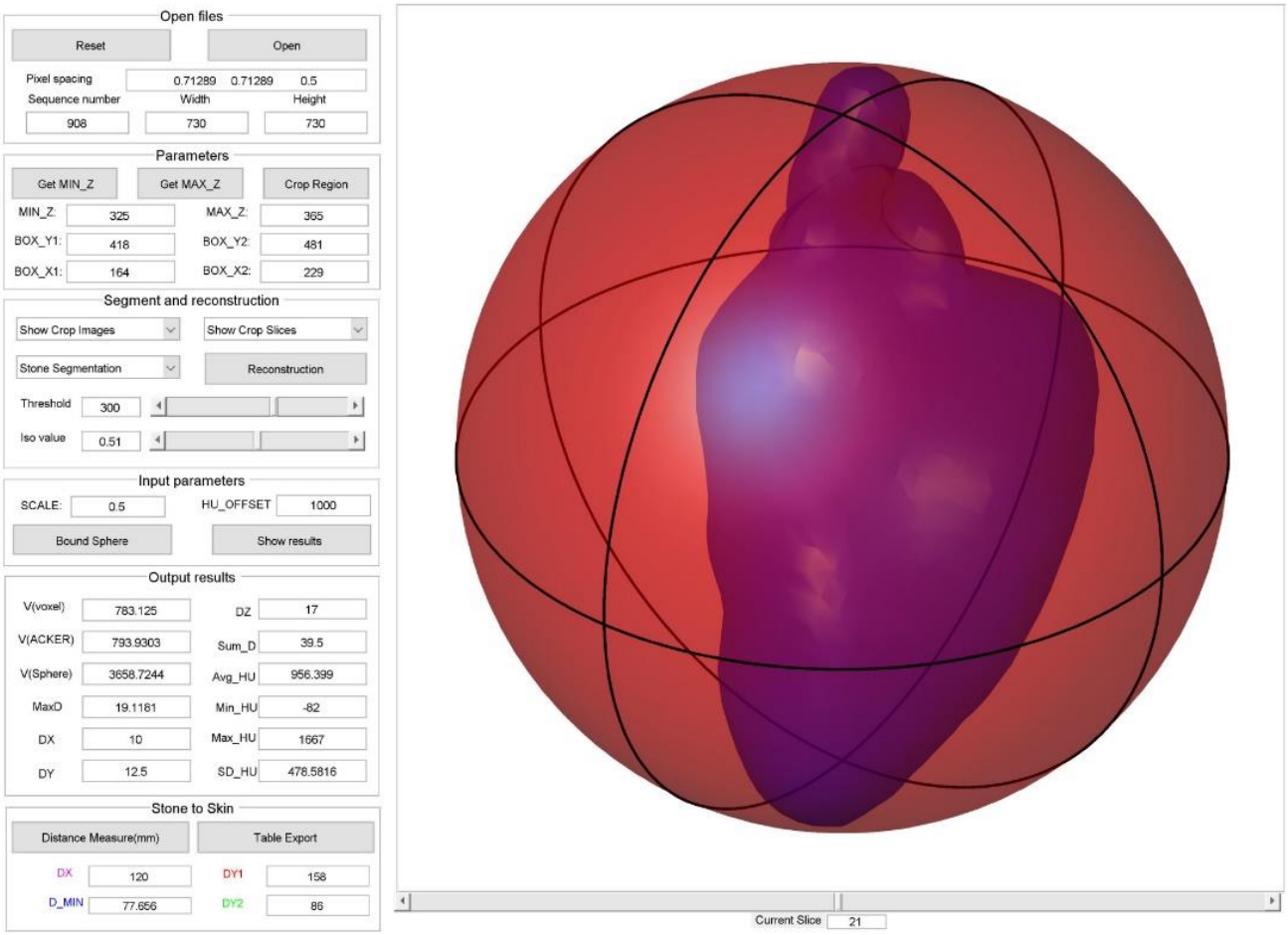

Fig. 4. User-friendly interface showing bounded sphere of index renal stone.

analysis program. If multiple stones were present, then a representative single stone was selected as our ROI. The parameters calculated for each ROI included volume (voxel, mm^3), maximum diameter (mm), largest diameter in *x*, *y*, and *z* dimensions (mm), cumulative diameter (mm), density (HU), and SSD. Volume was measured directly by summing all voxels within the stone, calculated using the formula for a sphere ($4/3\,\pi r^3$, where r is the maximum radius in any one direction), and the formula based on Ackermann's water displacement model [$0.6(\text{area})^{1.27}$, where area is calculated as πr^2 representing the area of a circle at the midpoint of the stone].[18] SSD was calculated automatically by identifying the distance in the *x* and *y* axis from the ROI to the skin surface with identification of a line representing the shortest distance to the skin in the posterior direction. This study was approved the Johns Hopkins Institutional Review Board with informed consent waived.

Results

A total of 55 patients were identified through the screening process with all patients verified to have a renal stone on imaging. Thus, the final study cohort consisted of 55 index renal stones. The mean volume calculated by voxel sum was 216.53 mm^3 (standard deviation [SD] ±616.19, range 1.50–4060.13). The mean volume calculated using the Ackermann's formula and for a sphere was 232.96 mm^3 (SD ±702.65, range 1.24–4074.04) and 1214.63 mm^3 (SD ±4233.41, range 1.77–25,246.40), respectively. The mean largest diameter in any one direction was 6.95 mm (SD ±7.31, range 1.50–36.40). The maximum density of the stones ranged from 164 to 1725 HU. The mean SSD at the shortest possible point was 14.19 cm (SD ± 6.13, range 6.67–31.28). The calculated parameters for each individual stone are summarized in Table 1.

Discussion

In this study, we achieved our goal of developing a standalone platform with a simple easy-to-use interface, which would allow any user the ability to calculate a battery of clinically important urinary stone parameters from CT imaging at the POC. Unique to this study is that we have made this program freely available via direct download for use in clinical care or within the research community.

The importance of urinary stone parameters, such as stone size, density, and location, cannot be understated in helping urologists to appropriately counsel patients and then select the optimal treatment modality for stone removal. The American Urological Association Guideline on the Surgical Management of Stones provides an evidence-based framework for optimal clinical care using these parameters.[7,8] For example, we know that spontaneous stone passage rate dramatically decreases with increasing stone size and a more proximal location.[7–9] Similarly, for shockwave lithotripsy, stones that are large, dense, or located in an unfavorable location, such as in the distal or mid-ureter, or at an increased distance from the skin have lower rates of fragmentation than ureteroscopy.[7,8,19] Recently, stone volume has also demonstrated prognostic value in predicating a variety of clinically relevant outcomes like success with a trial of spontaneous passage and recurrent stone events after percutaneous nephrolithotomy.[16,20,21]

Despite the obvious value of knowing these renal stone parameters, typically stone size, often in only a single dimension is readily available or reported.[10] However, with CT now the de facto gold standard for renal stone imaging and 3D reformatting, computer-aided tools, and algorithms readily available across all major CT platforms,[22,23] it is no longer acceptable to rely only on the manual calculation of the largest dimension of the stone to make clinical decision. Instead, we must leverage these CT capabilities to make all clinically relevant renal stone parameters accessible at the POC.

In fact, this is not a new concept. It was first attempted in 1989 by Ackermann and colleagues,[18] where they developed a computer program to calculate stone volume based on a traced area of the stone from a radiograph. Since that time, our technology has substantially increased. It is now accepted that CT attenuation threshold segmentation algorithms can accurately and precisely measure stone parameters, particularly axial dimensions and volume.[15,17] Furthermore, automated calculations are significantly more reproducible and reliable than manual measurements with electronic calipers.[19]

Despite the growing literature on the value of automated stone parameter calculation, its use in routine clinical practice remains restricted. It is unlikely that this is due to a lack of availability of modern CT technology. Multidetector CT were first introduced in 1998.[24] With the introduction of these scanners, it became possible to capture the volumetric data necessary for multiplanar reformations and 3D reconstructions.[24] Since that time, the tools necessary for postprocessing have become commonplace.[22,23,25–27] However, the burden of performing postprocessing, extracting the data, and interpreting it still rests with the technologist and radiologist.[25] This is arguably the greatest barrier to adoption. However, as urologists, we are also at fault. Traditionally, we have not requested that urinary stone parameters be calculated as part of a stone protocol CT report. The first step to correcting this deficiency is to ask our radiology colleagues to make this a priority.

However, even if urinary stone parameters do become routinely reported as part of a stone protocol CT, there will still be a role for a POC calculation by the urologist. In fact, POC calculations are likely to be the norm, rather than exception. This is because many patients suffering from renal stone disease arrive to the urologist's office with a CT image in hand performed elsewhere, often during an acute visit in the emergency department. Furthermore, as surgeons we still like the ability to review our own films with the purpose of planning a safe and effective operative approach.

Therefore, to meet this need, we have developed a standalone freely available CT postprocessing program specifically designed with the urologist as the end user. The program features an easy-to-use point-and-click interface organized in a stepwise manner to facilitate postprocessing and automated calculations. There is an option for data exportation for research purposes or trending practice habits and outcomes such as stone-free rate. However, the strength of the program is rooted in its ability to automatically calculate all clinically relevant urinary stone parameters, such as volume, diameter in each plane, maximal diameter, sum diameter, average and peak density, and SSD. It will even calculate these parameters for branched irregularly shaped stones (Fig. 3).

Table 1. Individual Urinary Stone Measurements of the Validation Cohort

Patient No. (N=55)	*Volume (mm^3)*			*Diameter (mm)*					*Density (HU)*			SSD *(mm)*
	Voxel	*Ackermann's formula*	*Sphere formula*	*Maximum*	x	y	z	*Sum*	*Average*	*Maximum*	*SD*	*Minimum*
1	172.3	285.9	1095	12.79	9	9	9	27	544	1123	241	177
2	81	58.08	166.7	6.828	5.5	6	4	15.5	782	1725	452.3	107
3	719.3	578.2	2516	16.87	12	13	14	38.5	937	1587	449.5	107
4	55.13	38.37	102.2	5.8	5	4	5	13.5	577	1281	304.8	233
5	46.88	40.97	110.4	5.951	4.5	4	5	13	499	1056	243.6	120
6	22.63	48.27	134	6.348	6	4	2	11.5	406	821	200.8	137
7	14.5	14.1	31.32	3.911	3	3	3	8	441	982	251.7	125
8	1508	1148	5656	22.11	18	17	18	51.5	987	1494	398.7	116
9	3.625	2.982	4.998	2.121	2	2	1	4.5	276	486	114.1	96.1
10	10.25	11.44	24.46	3.601	3	2	3	7.5	402	936	214.6	147
11	1320	3144	18,588	32.87	14	28	25	66	718	1564	351.7	194
12	78.88	85.56	263.4	7.953	6	6	6	18	528	1273	284.5	206
13	17.25	20.14	47.71	4.5	3.5	3	3	9	399	769	155.8	89.2
14	2.75	3.961	6.991	2.372	1.5	2	2	4.5	258	361	61.52	98.3
15	12.25	8.104	16.28	3.144	2.5	3	2	7	473	1039	263.7	127
16	27.63	19.8	46.75	4.47	3.5	3	4	10	510	1151	278.4	190
17	44.38	55.45	157.8	6.705	3	6	4	13	478	966	222.4	247
18	5.5	3.627	6.299	2.291	2	2	2	5.5	320	586	128.3	70.5
19	5.75	5.836	11.05	2.763	2.5	2	2	6.5	299	487	92.18	223
20	13	8.746	17.81	3.24	2.5	3	2	7	445	965	236.5	100
21	17	18.27	42.51	4.33	3	3	3	9	386	732	171.9	76.4
22	70	197.1	705.6	11.05	8.5	8	5	21.5	530	1140	244.2	238
23	2.5	4.297	7.695	2.449	1.5	2	1	4.5	257	341	44.86	113
24	10.38	12.27	26.57	3.702	3.5	2	2	7	347	689	177.4	66.7
25	4060	4074	25,246	36.4	30	32	23	84	695	1320	253.6	313
26	5.625	3.847	6.754	2.345	1.5	2	2	5	304	560	120.8	161
27	32.5	24.08	58.93	4.828	4	4	4	11.5	467	972	204.9	171
28	8.625	7.836	15.65	3.103	2.5	3	1	6.5	380	831	188.1	79.8
29	409.6	290.3	1115	12.87	11	11	10	31.5	533	1247	247.9	112
30	16.5	14.34	31.95	3.937	3	3	3	8	439	1069	248.3	81.5
31	38.5	45.67	125.5	6.212	5	5	3	12.5	593	1313	316.9	161
32	2.625	2.222	3.531	1.889	1	2	1	3.5	220	286	37.35	106
33	93.13	99.53	314.9	8.441	8	5	4	16.5	596	1298	305.1	111
34	22	13.47	29.66	3.841	3	3	4	9	501	1184	284.6	95.2
35	541.9	488.9	2064	15.8	12	11	13	35.5	466	695	149.1	222
36	2.25	1.334	1.933	1.546	1	1	1	3	180	286	53.27	91.8
37	4.625	3.627	6.299	2.291	2	2	1	5	342	593	138.6	198
38	47.75	45.85	126.1	6.221	4.5	3	5	12.5	416	796	178.6	107
39	783.1	793.9	3659	19.12	10	13	17	39.5	956	1667	478.6	77.7
40	2.625	2.081	3.268	1.841	1.5	2	1	4	282	473	104.8	253
41	1.625	1.595	2.388	1.658	1.5	1	1	3	147	263	62.44	81.6
42	10.75	8.735	17.79	3.239	2.5	3	2	7	336	611	125.1	113
43	27.38	16.64	38.07	4.174	3	4	4	10.5	482	1193	335.4	166
44	1.5	1.436	2.109	1.591	1	1	1	3	121	164	24.65	74.3
45	18.25	11.98	25.83	3.668	3	3	3	8	482	1185	284.9	105
46	141.4	106.8	342.2	8.678	6.5	7	8	21.5	716	1534	384.3	158
47	1.75	1.595	2.388	1.658	1.5	1	1	3	130	179	29.78	84.9
48	5.25	3.9	6.862	2.358	2	2	2	5	288	547	136.6	252
49	14.75	25.32	62.53	4.924	4.5	3	2	9.5	357	714	146.6	92.9
50	5.625	3.774	6.601	2.327	2	2	1	5	335	657	160.9	115
51	15.13	15.85	35.96	4.095	3	4	3	9	433	972	217.1	121
52	10.38	9.547	19.76	3.354	2	3	2	6	328	513	93.05	112
53	769.1	461.7	1929	15.44	10	13	13	35.5	1009	1706	474.7	89.3
54	1.75	1.236	1.767	1.5	1	1	1	2.5	198	389	91.03	247
55	552.5	418.6	1718	14.86	10	12	12	33.5	670	1286	271.8	243

HU=Hounsfield units; SD=standard deviation; SSD=skin-to-stone distance.

There are several limitations in our study. First, we did not correlate the automated calculations against a known benchmark such as a phantom model to confirm their accuracy or reproducibility. However, others have consistently demonstrated the accuracy and precision of attenuation threshold segmentation algorithms to measure stone parameters, particularly axial dimensions and volume.[15,17] Second, we did not examine how each individual parameter may influence clinical outcomes. However, none of the included parameters are novel but instead were explicitly selected because of their well-documented influence on clinical outcomes in urinary stone disease.[7,8] Third, we have not tested this program on other CT manufacturers, across differing CT protocols, or outside our institution, and thus, it may not be as easy to use or integrate or applicable to other practice environments. However, we are making this software freely available, and it is our hope that others will confirm its utility and ease of use.

Conclusions

In this study, we achieved our goal of developing a standalone platform with a simple easy-to-use interface, which would allow any user the ability to calculate a battery of clinically important urinary stone parameters from CT imaging at the POC. Unique to this study is that we have made this program freely available via direct download for use in clinical care or within the research community. We hope that this program will become another tool in the armamentarium of the urologist to maximize clinical outcomes in patients with urinary stone disease.

Acknowledgments

The software program described in this article was written primarily by the author Pan Li. We thank Mr. and Mrs. Jerry and Helen Stephens for their continued support of kidney stone disease research at the Brady Urological Institute. This study was approved by the Johns Hopkins Institutional Review Board with informed consent waived.

Disclaimer

The software program described in this article is available online (http://urobotics.urology.jhu.edu/share/rsm). The program is made available by the Johns Hopkins University (JHU) solely for personal, noncommercial, teaching, and educational use. JHU owns all intellectual property related to this software. This program is not a medical device, and the safety and efficacy of this program to diagnose health conditions has not been evaluated by the U.S. Food and Drug Administration. This program is provided for educational and informational purposes only and does not and should not be construed to provide health-related or medical advice, or clinical decision support, or to support, replace the diagnosis, recommendation, advice, treatment, or decision by an appropriately trained and licensed physician, including, without limitation, with respect to any life-sustaining or lifesaving treatment or decision. This program does not create a physician–patient relationship between JHU and any individual. The program may not be purchased, downloaded, accessed, or used by anyone under the age of 13. By downloading, accessing, viewing, or using the program, you, the user, agree to use the program solely in accordance with the foregoing, as terms and conditions of the end user license agreement between you and JHU.

Author Disclosure Statement

J.B.Z. is a consultant for Visible Health, Inc., but this research was not related. P.L., W.W.L., R.G., S.K., D.S., and E.F. declare that they have no competing financial interests. G.F. is an employee of the Siemens Medical Solutions USA, but this research was not sponsored by or related to his employment. B.R.M. is a consultant for the Boston Scientific Corporation, but this research was not related.

References

1. Scales CD, Jr, Smith AC, Hanley JM, Saigal CS; Urologic Diseases in America Project. Prevalence of kidney stones in the United States. Eur Urol 2012;62:160–165.
2. Rule AD, Lieske JC, Li X, Melton LJ, 3rd, Krambeck AE, Bergstralh EJ. The ROKS nomogram for predicting a second symptomatic stone episode. J Am Soc Nephrol 2014; 25:2878–2886.
3. Litwin M, Saigal C. Table 9-33. Use of imaging procedures in Medicare beneficiaries for evaluation of urinary tract stones. In: United States Department of Health and Human Services PHS, National Institute of Health, National Institute of Diabetes and Digestive and Kidney Diseases, eds.: Urologic Diseases in America. Compendium. Washington, DC: US Government Printing Office, 2012, p. 345.
4. Fulgham PF, Assimos DG, Pearle MS, Preminger GM. Clinical effectiveness protocols for imaging in the management of ureteral calculous disease: AUA technology assessment. J Urol 2013;189:1203–1213.
5. Ziemba JB, Matlaga BR. Guideline of guidelines: Kidney stones. BJU Int 2015;116:184–189.
6. Hyams ES, Bruhn A, Lipkin M, Shah O. Heterogeneity in the reporting of disease characteristics and treatment outcomes in studies evaluating treatments for nephrolithiasis. J Endourol 2010;24:1411–1414.
7. Assimos D, Krambeck A, Miller NL, et al. Surgical management of stones: American Urological Association/Endourological Society Guideline, PART I. J Urol 2016;196: 1153–1160.
8. Assimos D, Krambeck A, Miller NL, et al. Surgical Management of Stones: American Urological Association/Endourological Society Guideline, PART II. J Urol 2016;196: 1161–1169.
9. Coll DM, Varanelli MJ, Smith RC. Relationship of spontaneous passage of ureteral calculi to stone size and location as revealed by unenhanced helical CT. AJR Am J Roentgenol 2002;178:101–103.
10. Patel SR, Nakada SY. Quantification of preoperative stone burden for ureteroscopy and shock wave lithotripsy: Current state and future recommendations. Urology 2011;78: 282–285.
11. Finch W, Johnston R, Shaida N, Winterbottom A, Wiseman O. Measuring stone volume—Three-dimensional software reconstruction or an ellipsoid algebra formula? BJU Int 2014;113:610–614.
12. Patel SR, Stanton P, Zelinski N, et al. Automated renal stone volume measurement by noncontrast computerized tomography is more reproducible than manual linear size measurement. J Urol 2011;186:2275–2279.
13. Alluri K, Joshi PH, Henry TS, Blumenthal RS, Nasir K, Blaha MJ. Scoring of coronary artery calcium scans:

History, assumptions, current limitations, and future directions. Atherosclerosis 2015;239:109–117.
14. Demehri S, Steigner ML, Sodickson AD, Houseman EA, Rybicki FJ. Silverman SG. CT-based determination of maximum ureteral stone area: A predictor of spontaneous passage. AJR Am J Roentgenol 2012;198:603–608.
15. Demehri S, Kalra MK, Rybicki FJ, et al. Quantification of urinary stone volume: Attenuation threshold-based CT method—A technical note. Radiology 2011;258:915–922.
16. Bandi G, Meiners RJ, Pickhardt PJ, Nakada SY. Stone measurement by volumetric three-dimensional computed tomography for predicting the outcome after extracorporeal shock wave lithotripsy. BJU Int 2009;103:524–528.
17. Liden M, Andersson T, Broxvall M, Thunberg P, Geijer H. Urinary stone size estimation: A new segmentation algorithm-based CT method. Eur Radiol 2012;22:731–737.
18. Ackermann D, Griffith DP, Dunthorn M, Newman RC, Finlayson B. Calculation of stone volume and urinary stone staging with computer assistance. J Endourol 1989;3:355–360.
19. Perks AE, Schuler TD, Lee J, et al. Stone attenuation and skin-to-stone distance on computed tomography predicts for stone fragmentation by shock wave lithotripsy. Urology 2008;72:765–769.
20. Selby MG, Vrtiska TJ, Krambeck AE, et al. Quantification of asymptomatic kidney stone burden by computed tomography for predicting future symptomatic stone events. Urology 2015;85:45–50.
21. Zorba OU, Ogullar S, Yazar S, Akca G. CT-based determination of ureteral stone volume: A predictor of spontaneous passage. J Endourol 2016;30:32–36.
22. CT Advanced Visualization: GE Healthcare. 2018. Available at: http://www3.gehealthcare.com/en/products/categories/advanced_visualization/computed_tomography_imaging_software (accessed March 3, 2018).
23. syngo.via Reading as it should be: open and ready: Siemens Healthineers. 2018. Available at: https://www.healthcare.siemens.com/medical-imaging-it/advanced-visualization-solutions/syngovia (accessed March 3, 2018).
24. Dale J, Gupta RT, Marin D, Lipkin M, Preminger G. Imaging advances in urolithiasis. J Endourol 2017;31:623–629.
25. Mezrich R, Juluru K, Nagy P. Should post-processing be performed by the radiologist? J Digit Imaging 2011;24:378–381.
26. Mujika KM, Mendez JAJ, de Miguel AF. Advantages and disadvantages in image processing with free software in radiology. J Med Syst 2018;42:36.
27. Valeri G, Mazza FA, Maggi S, et al. Open source software in a practical approach for post processing of radiologic images. Radiol Med 2015;120:309–323.

Address correspondence to:
Justin B. Ziemba, MD
Division of Urology, Department of Surgery
Perelman School of Medicine
University of Pennsylvania
3 West Perelman Center for Advanced Medicine
3400 Civic Center Boulevard
Philadelphia, PA 19104

E-mail: justin.ziemba@uphs.upenn.edu

Abbreviations Used

3D=three dimensional
CT=computed tomography
HU=Hounsfield units
POC=point-of-care
ROI=region of interest
SD=standard deviation
SSD=skin-to-stone distance